Talanta 125 (2014) 7–13

Contents lists available at ScienceDirect

Talanta

journal homepage: www.elsevier.com/locate/talanta

# Introducing a new method for evaluation of the interaction between an antigen and an antibody: Single frequency impedance analysis for biosensing systems

Burcu Özcan, Burçak Demirbakan, Gülden Yeşiller, Mustafa Kemal Sezgintürk*

*Namık Kemal University, Faculty of Science and Arts, Chemistry Department, Biochemistry Division, Tekirdağ, Turkey*

ARTICLE INFO

*Article history:*
Received 7 December 2013
Received in revised form
20 February 2014
Accepted 25 February 2014
Available online 6 March 2014

*Keywords:*
Single frequency impedance
Parathyroid hormone
Anti-parathyroid hormone
Biosensor
Parathyroidism
Biomarker

ABSTRACT

This paper illustrates the application of an antibody, anti-parathyroid hormone (anti-PTH), as a bioreceptor in a biosensor system for the first time, and demonstrates how this biosensor can be used in parathyroid hormone (PTH) determination. The interaction between the biosensor and parathyroid hormone was firstly investigated by a novel electrochemical method, single frequency impedance analysis. The biosensor was based on the gold electrode modified by cysteine self-assembled monolayers. Anti-PTH was covalently immobilized onto cysteine layer by using an EDC/NHS couple. The immobilization of anti-PTH was monitored by cyclic voltammetry and electrochemical impedance spectroscopy techniques. The performance of the biosensor was evaluated in terms of linearity, sensitivity, repeatability and reproducibility, after a few important optimization studies were carried out. In particular, parathyroid hormone was detected within a linear range of 10–60 fg/mL. Kramers–Kronig transform was also performed on the impedance data. The specificity of the biosensor was also evaluated. The biosensor was validated by using a complementary reference technique. Lastly the developed biosensor was used to monitor PTH levels in artificial serum samples.



## 1. Introduction

Parathyroid hormone (PTH) is secreted from cells of parathyroid glands and has a vital role in the regulation of calcium and phosphorous concentration in extracellular fluid [1–3]. Basically PTH accomplishes the regulator role by stimulating at least three processes: mobilization of calcium from bone, enhancing absorption of calcium from the small intestine, and suppression of calcium loss in urine [4–9]. PTH has a very powerful influence on bones to release calcium ions when the extracellular calcium concentrations are decreased [10,11]. The changes in secretion of parathyroid hormone should be recognized as causes of serious diseases such as hyperparathyroidism due to a parathyroid tumor which secretes PTH without proper regulation [12,13], or hypoparathyroidism which results in lowered levels of calcium and increased concentrations of phosphorus in blood [14–16]. There is no doubt that both hyperparathyroidism and hypoparathyroidism result in serious cases.

Electrochemical impedance spectroscopy (EIS) is an efficient method to investigate chemical and physical processes. Identification of membranes, biosensor characterization and fabrication could be monitored by EIS, effectively. Conversely enzyme–substrate interactions, after antigen–antibody, receptor–ligand, or DNA–DNA interactions which have no catalytic reaction, could be successively monitored by EIS [17–19]. Impedimetric biosensors based on self-assembled monolayers (SAM) and carbodiimide activation have been reported by several research groups [20–24]. Immunosensors that used conductive polymer films based on electrochemical impedance spectroscopy were reported [25–28]. Recently different types of biosensing techniques based on impedance such as electrodeposition of nanometer-sized hydroxyapatite [29], phenomena of polymer degradation [30], molecular imprinted polymers [31], and magnetic nanobeads[32] have also been reported.

In this study two important impedance parameters were also studied: Kramers–Kronig Trasform and single frequency impedance measurements. The Kramers–Kronig relations are integral equations that constrain the real and imaginary components of complex quantities for systems that satisfy conditions of linearity, causality, and stability [33–35]. In principle, the Kramers–Kronig relations can be used to determine whether the impedance spectrum of a given system has been influenced by bias errors caused, for example, by instrumental artifacts or time-dependent phenomena. This information is critical to the analysis and interpretation of electrochemical impedance spectroscopy data due to difficulties with their applications [35]. The Kramers–Kronig

* Corresponding author.
*E-mail addresses:* msezginturk@hotmail.com, msezginturk@nku.edu.tr (M.K. Sezgintürk).

http://dx.doi.org/10.1016/j.talanta.2014.02.067
0039-9140 

relations have been applied to electrochemical systems by direct integration of the equations, by experimental observation of stability and linearity, by regression of specific electrical circuit models, and by regression of generalized measurement models [36,37]. Direct integration of the Kramers–Kronig relations involves calculating one component of the impedance from the other, e.g., the real component of impedance from the measured imaginary component. The result is compared to the experimental values obtained [35].

The other parameter, single frequency impedance measurement, was also applied to the new biosensor system in order to characterize the interaction between PTH and anti-PTH for the first time. Single frequency impedance measures the impedance at a fixed frequency versus time. Consequently it should be possible to control the experiment with a repeat time and a total time.

The objective of this work is to fabricate a biosensor for sensitive and practical analysis of human parathyroid hormone. The proposed biosensor based on anti-PTH is the first biosensor system for this purpose in the literature. A self-assembled monolayer strategy for introducing an immobilization platform on the gold electrodes is reported in the present study. Anti-PTH antibody is covalently attached to the SAM of cysteine by the help of the couple of 1-ethyl-3-(3-dimehylaminopropyl)carbodiimide (EDC) and N-hydroxysuccinimide (NHS). The proposed biosensor can detect the concentrations of PTH as low as subpicogram scales.

## 2. Experimental

### 2.1. Materials and instrumentation

All reagents were of analytical grade unless stated otherwise and were purchased from Sigma-Aldrich (St.Louis, MO, USA). Parathyroid hormone and anti-parathyroid hormone were purchased from Sigma-Aldrich (St.Louis, MO, USA). PTH and anti-PTH portions were prepared at certain concentrations and were stored at $-20\,^{\circ}C$ until use. Artificial serum solution was prepared by using 4.5 mM KCl, 5 mM $CaCl_2$, 1.6 mM $MgCl_2$, 4.7 mM D(+)-glucose, 2.5 mM urea, 0.1% human serum albumin, and 145 mM NaCl.

A three-electrode system, consisting of a gold working electrode (with a surface area of 2.01 $mm^2$), Ag/AgCl (saturated KCl) reference electrode and a Pt counter-electrode, was accommodated in a 5-mL electrochemical cell (all electrodes were obtained from iBAS, Warwickshire, UK). Electrochemical experiments were performed using a Gamry Reference 600 Potentiostat/Galvanostat, (Gamry Instruments, Warminster, USA) interfaced with a PC via an EChem Analyst containing physical electrochemistry, pulse voltammetry, and electrochemical impedance spectroscopy softwares (Gamry Instruments, Warminster, USA). In all electrochemical experiments a faraday cage (from iBAS, Warmickshire, UK) was used to block out external static electric fields.

### 2.2. Modification of the gold electrodes by cysteine SAM

Prior to modification each of the gold electrodes was polished with 0.05 μm $Al_2O_3$ powder and then washed ultrasonically in deionized water for 5 min to remove alumina particles. Then the electrodes were immersed into Piranha ($H_2O_2/H_2SO_4$, 30/70, v/v) solution for 3 min. Following that, the electrodes were washed with ultra-pure water by immersion into water 20 times. In the next step, the surfaces of the electrodes were dried by pure argon stream. This polishing and cleaning procedure was repeated before every electrode preparation step. Clean gold electrodes were immediately immersed into cysteine solution (0.05 M, in pure ethanol) overnight. After this period, it was rinsed with ethanol and gently dried with argon stream.

### 2.3. Covalent attachment of anti-PTH on cysteine modified electrodes

For anti-PTH immobilization, EDC was used as a heterobifunctional cross-linker. N-hydroxysuccinimide (NHS) was used in conjunction with the crosslinker EDC. Gold electrodes modified with cysteine SAM were dipped in a glass bottle containing EDC/NHS solution (0.04 mM EDC, 0.01 mM NHS) for an hour in a dark ambient. Later, gold electrodes were washed with ultra-pure water gently and then dried by pure argon stream again. At the last step, 5 μL of anti-PTH portion was applied to the active electrode surface by a pipette. The electrode was allowed to incubate for an hour in a moisture medium. Finally the electrode was immersed into ultra-pure water to remove physically adsorbed anti-PTH molecules. Bare gold electrodes and the modified electrodes were denoted as Au, Au/Cys, Au/Cys/Anti-PTH, Au/Cys/Anti-PTH/BSA, and Au/Cys/Anti-PTH/BSA/PTH.

### 2.4. Electrochemical procedures and parameters

Cyclic voltammetry was used to characterize SAM formation on bare gold electrodes and modified electrodes with different layers. The potential was varied between 0 and 500 mV (step size: 20 mV, scan rate: 50 mV/s) in the presence of 5 mM $K_3[Fe(CN)_6]/K_4[Fe(CN)_6]$ (1:1) solution which served as a redox probe containing 0.1 M KCl. For electrochemical impedance studies, an alternating wave with an amplitude of 10 mV was applied to the electrode.

In the potentiostatic mode, the electrochemical impedance experiments were done at a fixed DC potential of 0 V. The redox couple used for impedance studies was the same as that used for cyclic voltammetry. Impedance spectra were collected in the frequency range between 10,000 and 0.05 Hz.

## 3. Results and discussion

### 3.1. Electrochemical investigation of step-by-step anti-PTH immobilization

Electrochemical properties of the biosensor were investigated after each assembly step. The scale of electrically insulation was examined with the frequently used redox couple ($K_3[Fe(CN)_6]$) through the electron transfer kinetics of $[Fe(CN)_6]^{4-}/[Fe(CN)_6]^{3-}$ redox reactions using cyclic voltammetry and electrochemical impedance spectroscopy techniques in the electrolyte solution.

Fig. 1A shows cyclic voltammograms of the modified electrode. In the investigation of electron transfer rate of the modified electrodes, cyclic voltammetry is a very powerful tool. As known, the variations in oxidation and reduction peak currents in cyclic voltammograms related with different electrode surfaces can be theoretically attributed to electron transfer rates or charge transfer resistances [38,39]. Therefore, cyclic voltammetry was firstly used in the investigation of the peak currents of redox probe and then EIS was utilized for the characterization of the stepwise changes of the surfaces of the biosensor by interpreting the charge transfer resistances. In Fig. 1, characteristic curve related to bare gold electrode can be observed easily. First of all, it was reported that when gold electrodes were immersed into the cysteine solution, a thermodynamically favored bond was formed between the gold and the thiol [40]. Moreover, it could be seen that self-assembling of cysteine on clean gold surface did not change the oxidization and reduction peaks of the redox probe, considerably. When the EDC/NHS couple was reacted with cysteine, the peak current values of the redox probe increased slightly. The results in Fig. 1A reveal that voltammetric characteristics of the redox probe are slightly inflenced by the modification of electrode surface with self-assembling of cysteine and by its activation with EDC/NHS couple.

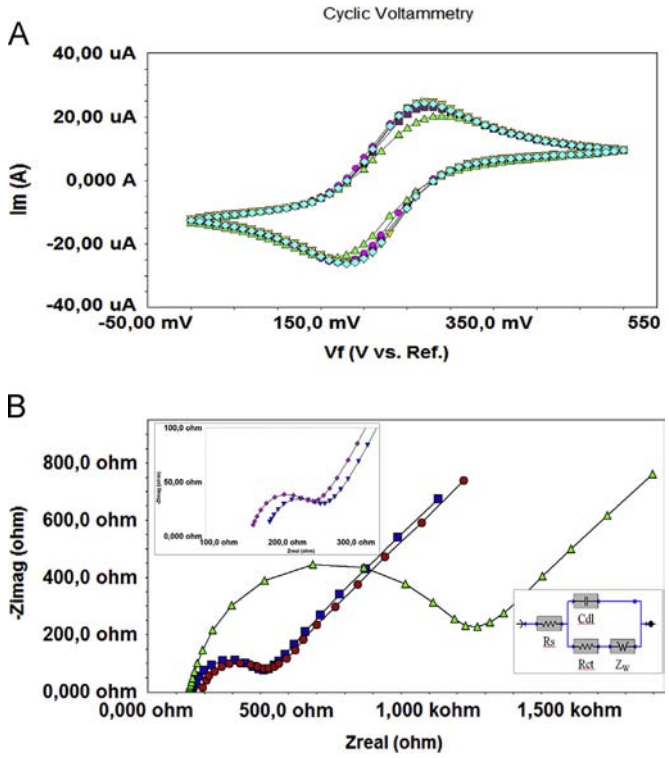


**Fig. 1.** Electrochemical characterization of anti-PTH biosensor [ (A) cyclic voltammograms related with anti-PTH immobilization by covalent attachment and (B) electrochemical impedance spectra of anti-PTH immobilization steps; -●-●-: bare gold electrode, -▼-▼-: Au/Cys, -◆-◆-: Au/Cys/EDC–NHS, -■-■-: Au/Cys/EDC–NHS/anti-PTH, -▲-▲-: Au/Cys/EDC–NHS/anti-PTH/BSA].

Probably, this result may also show self-assembling of cysteine. Moreover its activation by EDC/NHS did not change the electron-transfer rate constant. Further the redox peaks were decreased when anti-PTH was linked covalently to the electrode surface via the reaction with amine-reactive NHS ester. Covalent attachment of anti-PTH on the surface enhanced the insulating property of the electrode surface. Blocking of free active ends with bovine serum albumin (BSA) further decreased the redox peaks because of insulating properties of BSA protein attached to the electrode surface. The cyclic voltammetry experiments confirmed that cysteine and anti-PTH were successfully assembled on the gold surface. Also the results illustrated that the immobilization of anti-PTH and BSA blockage insulated the electrode surface.

For the analysis of charge transfer resistance, $R_{ct}$, EIS can be effectively used. The representative Nyquist plots of EIS spectra related to different layers of the modified electrode can be seen in Fig. 1B. Typically, each impedance spectrum has a semicircular portion and a linear portion. The semicircle portion observed at high frequencies corresponds to the electron transfer limited process of $[Fe(CN)_6]^{3-/4-}$, whereas the linear part represents the diffusion limited process. The diameter of the semicircle is used for calculation of charge transfer resistance at any electrode surface. An equivalent circuit can be modeled for the measured EIS data as shown in the inset of Fig. 1B. This equivalent circuit model includes an ohmic resistance ($R_s$) regarding the resistance of the electrolyte solution between the gold electrode and the reference electrode, charge transfer resistance, $R_{ct}$, the double layer capacitance connected with the capacitance of the complex bioactive layer, and the Warburg impedance, $Z_w$, representing the normal diffusion to the electrode surface through the complex layer. In an electrochemical system, the resistance of electrolyte solution is related to the bulk properties of the electrolyte solution. Besides, Warburg impedance represents the diffusion of the redox probe through the electrode surface. Nevertheless, these two components are not influenced by chemical modifications performed at the electrode surface. On the other hand, for the presented biosensor system, it was shown that $R_s$ and $Z_w$ were not affected by the procedures related to immobilization of anti-PTH. However, especially $R_{ct}$ was strictly influenced by the dielectric and insulating features at the electrode/electrolyte interface. It is obvious that the magnitude of $R_{ct}$ slightly decreases by self-assembling cysteine and its EDC/NHS activation. The $R_{ct}$ values for cysteine and EDC/NHS activation were 173.5 and 179.5 Ω, respectively. These lower $R_{ct}$ values than those of bare gold electrode (303.4 Ω) imply that the electron transfer process $[Fe(CN)_6]^{3-/4-}$ on the modified gold surface is relatively fast compared to that for the bare gold electrode. The covalent attachment of anti-PTH on the electrode surface generates a protein layer that introduces a barrier to the interfacial electron transfer, which is clearly indicated by the significant increase of $R_{ct}$ of the electrode to the value 2453 Ω. The blocking of free active ends by BSA results in a further increase of $R_{ct}$, due to the rather insulating effect of BSA on the modified electrode surface. The impedance experiments reveal the good agreement between the measured impedance and the fitting curve indicates that the equivalent circuit model used for impedance evaluations is suitable and meaningful for this biosensor system. Nevertheless, the equivalent circuit model can be successfully used to fit the impedance spectroscopy data and extract the value of $R_{ct}$.

### 3.2. Optimization of the biosensor

The experimental conditions affecting the biosensor response were studied in terms of effect of cysteine concentration, anti-PTH concentration, anti-PTH incubation period, PTH incubation period, and best fitting frequency used in single frequency impedance study.

In order to establish the effect of cysteine concentration on the response of the present biosensor, cysteine solutions with different concentrations were utilized for the construction of biosensors. For this purpose, 10 fg/mL PTH standard solutions were separately analyzed by biosensors fabricated by using different cysteine solutions (0.01, 0.025, 0.05, and 0.075 M, in ethanol). The results are given in Fig. 1S, Supplementary material.

As shown in Nyquist plots in Fig. 1S, it was found that the highest charge transfer value was obtained with 0.05 M cysteine solution. $R_{ct}$ values related to different Cys concentrations were 3213, 3317, 4489, and 2959 Ω, correspondingly. This trend of decreasing sensitivity to PTH with increasing cysteine loading was expected. Higher concentrations of cysteine (0.075 M) resulted in denser immobilization of anti-PTH. As the density of anti-PTH increased, $R_{ct}$ from this layer increased, eventually blocking nearly all electron transfer. This prevented the subsequent binding of PTH from significantly changing the $R_{ct}$ as the anti-PTH layer had already blocked the vast majority of charge transfer to the surface.

Hence, taking into account this response profile, 0.05 M cysteine concentration was chosen as the optimal one to perform further experiments.

The effect of the anti-PTH concentration on the formation of biosensor recognition layer was studied by investigating three biosensors prepared from solutions including 0.1, 2.5, and 5 ng/μL anti-PTH. The impedance spectra related to different biosensors are shown in Fig. 2S, Supplementary material.

It was observed that an increase in the amount of anti-PTH resulted in an increase in $R_{ct}$. This could be an expected result because the more the anti-PTH antibody, the higher the charge transfer resistance. Consequently, the amount of PTH bound to the biosensor surface increased with increasing anti-PTH amount; accordingly the highest charge transfer resistance was recorded when 5 ng/μL of anti-PTH was utilized. Anti-PTH concentrations

higher than 5 ng/μL were not tested to prevent increased cost of a biosensor.

Another parameter that should be optimized is the optimization period for immobilization of anti-PTH antibody. The optimum incubation period was studied by incubating the biosensor with anti-PTH solution for different periods (30, 60, and 90 min). The results revealed that there were slight differences among the anti-PTH incubation periods tested. The charge transfer resistances obtained with different incubation periods were 2937, 2963, and 3483 Ω, correspondingly. Moreover, although the highest impedance value was obtained after a period of 90 min, evaluation of the PTH calibration graphs revealed that meaningful response was obtained by performing 60 min of incubation period.

Finally, another crucial factor was to study optimum incubation period for the interaction between anti-PTH and PTH which was required to carry out the binding process.

In order to determine optimum interaction period, different incubation periods (15, 30, 45, and 60 min) were used in the biosensor operation. The results can be seen in Fig. 3S, Supplementary material.

Prolonging incubation period up to 60 min resulted in an increase in the charge transfer resistance. Incubation periods longer than 60 min were not observed because of possible evaporation of anti-PTH solution injected onto the biosensor surface. Moreover extending incubation periods for antibody–antigen interaction to more than 60 min is generally not favored. In addition, incubation periods should be different with certain antibodies but in most studies they are between 30 min and 60 min for antigen–antibody interaction. If anti-PTH and PTH interactions' durations are evaluated in terms of total measurement period, the short period for the interaction process should be favorable. Finally, according to the results obtained, it was efficient to incubate PTH for an hour.

An optimization study was also performed to investigate the best fitting frequency used in single frequency measurements. First of all, in order to conclude which frequency could be used, and because Bode plots provide the impedance data as a function of frequency, Bode plots have been analyzed carefully. A sample of Bode plot related with our biosensor system is given in Fig. 2A.

As can be seen from Fig. 2A, a dramatic increase was observed in the frequency range of 10–100 Hz. Consequently we tested five different frequencies (10, 50, 80,100, and 1000 Hz) to evaluate the effect of frequency on single frequency measurements. Fig. 2B shows the variations in charge transfer resistances with changing single frequency values. According to these observations the optimum frequency value was 100 Hz. As a conclusion single frequency impedance measurements were carried out by using the frequency of 100 Hz, as can be found in the following section.

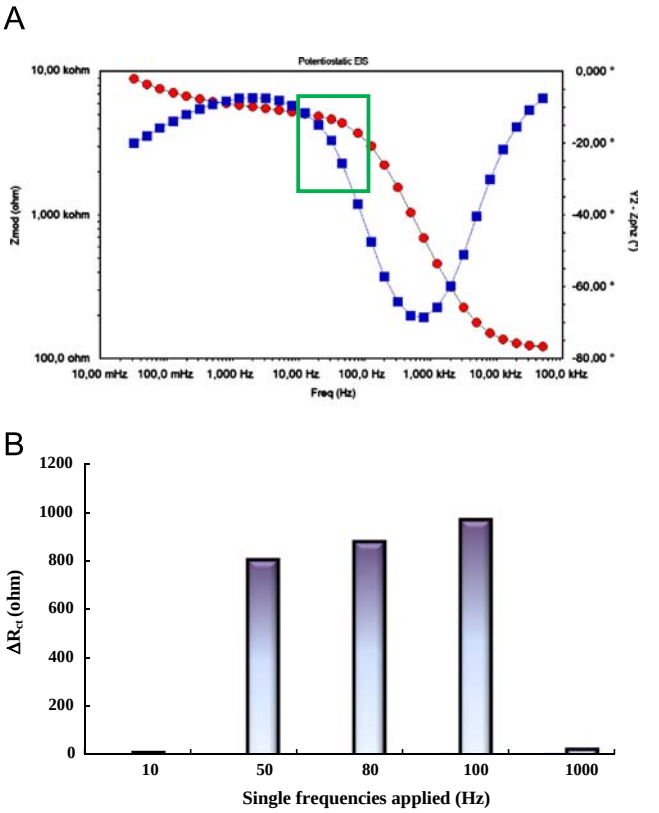


**Fig. 2.** Optimization of the frequency applied for the single frequency impedance measurement. (A) Bode plot for the evaluation of the optimum frequency used in single frequency impedance. (B) Impedance values obtained at different frequencies.

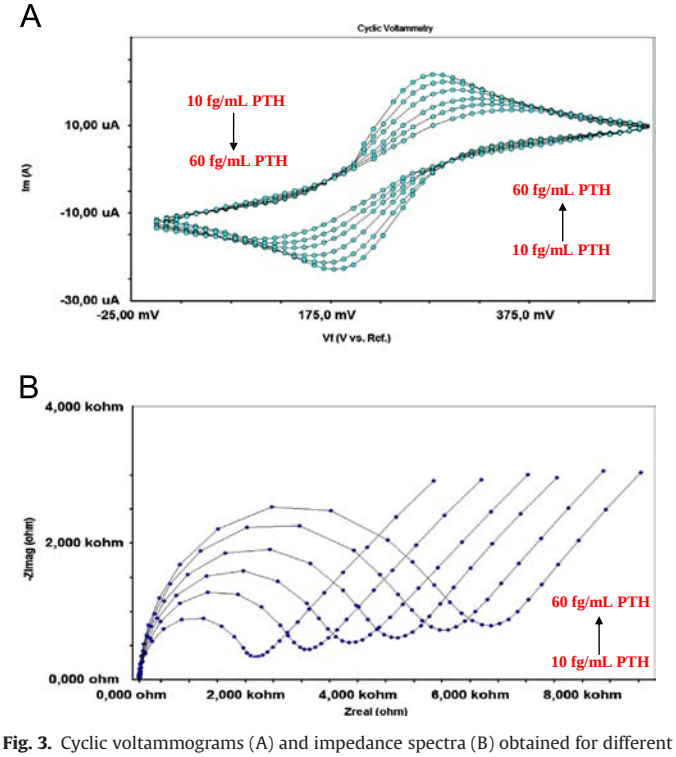


**Fig. 3.** Cyclic voltammograms (A) and impedance spectra (B) obtained for different concentrations of PTH by the present biosensor.

### 3.3. *Analytical characteristics of the biosensor*

PTH biosensors were further characterized with regard to its linear range, reproducibility and repeatability.

In the given study, electrochemical impedance spectroscopy was successfully performed to determine the amount of redox probe associated with changes in the charge transfer resistance at the anti-PTH biosensor. To obtain PTH calibration curves the absolute impedance values were utilized. The impedance variations were calculated by the following simple equation:

$$\Delta R_{ct} = R_{ct(PTH)} - R_{ct(BSA)}$$

where $R_{ct(PTH)}$ is the value of the charge transfer resistance after anti-PTH is coupled with PTH, while $R_{ct(BSA)}$ is the value of the charge transfer resistance when anti-PTH is immobilized on electrode surface. As can be seen from Fig. 3A, peak currents decreased with an increase in the concentrations of PTH standard solutions.

Fig. 3B shows the Nyquist plots' evaluation of the proposed biosensor for different PTH concentrations. It was revealed that the

semi-circle diameter in the Nyquist plots increased with increasing PTH concentrations. Moreover, low frequencies could be used for concentration dependent measurements. The increment of PTH concentration increased the charge transfer resistance, achieving a linear range between 10 fg/mL and 60 fg/mL. The results revealed that the presented anti-PTH biosensor allowed determining PTH in an extremely sensitive manner. A standard calibration graph for PTH was drawn by the help of the changes in charge transfer resistances after PTH applications. The calibration curve is given in Fig. 4. An immunoassay for the detection of PTH using actuated magnetic particle labels, which are measured with a giant magneto-resistive biosensor, was reported[41]. For the measurement of PTH, a detection limit in the 10 pM range was obtained with a total assay time of 15 min when 300 nm particles were used. Moreover it was also reported that the same sensitivity was achieved in 5 min when 500 nm particles were used. If 500 nm particles were employed in a 15-min assay, then 0.8 pM (7600 fg/mL) of PTH was detectable. A commercially available immunoassay (EIA) test kit can be frequently used by the laboratories. This product is an in vitro quantitative assay for detecting PTH based on the principle of competitive enzyme immunoassay. The minimum detectable concentration of PTH is 1.27 pg/mL. Moreover the cost of one well of the EIA kit is approximately 6 euros. However the cost of one biosensor is about just 10 cents.

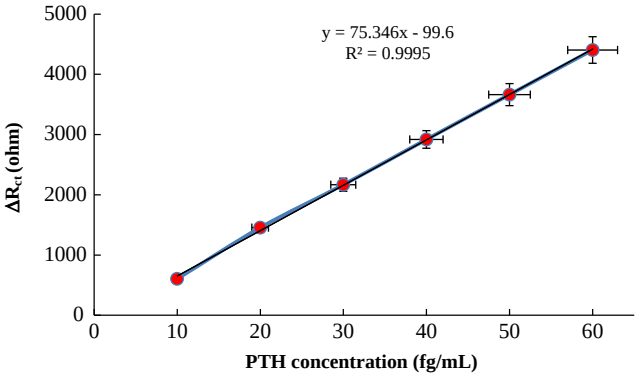


**Fig. 4.** PTH calibration curve obtained by the present anti-PTH based biosensor.

The reproducibility of the present anti-PTH biosensor was approved by using different biosensors fabricated via the same set of procedure for PTH analysis10 times. The results showed that the proposed biosensor reported here can be reproducibly utilized for PTH detection and quantification. The linear detection ranges of 10 biosensors for PTH were the same: between 10 fg/mL and 60 fg/mL. The results can be seen in Table 1.

Repeatability is another factor which should be determined in detail. The repeatability of anti-PTH based biosensor should be defined as the degree of a single biosensor to which it could be used continually for a series of measurements with the same concentration of PTH. Charge transfer resistances were recorded when the biosensors were consecutively exposed to a 10 fg/mL PTH standard solution 6 times. The repeatability of the measurements was very good considering that the correlation coefficient on measurements was 5.28%, and the average value and standard deviation were calculated as 10.21 fg/mL and $\pm$0.54 fg/mL, respectively.

For the present anti-PTH based biosensor, performance of the Kramers–Kronig transforms of the real part of the experimental data was used to calculate the imaginary part of a linear, stable, and causal circuit. Likewise, the imaginary portion of the experimental data was used to calculate the real part of a linear, stable,

**Table 1**
The results for Kramers–Kronig transforms, reproducibility, and the sample analysis.

| Biosensor surfaces | | Goodness of fit values | |
|---|---|---|---|
| *Kramers–Kronig transforms for different layers of the anti-PTH based biosensor* | | | |
| Bare gold electrode | | 27.5 | |
| Au/Cys | | 0.774 | |
| Au/Cys/EDC–NHS | | 4.136 | |
| Au/Cys/anti-PTH | | 0.588 | |
| Au/Cys/anti-PTH/BSA | | 7.478 | |
| Au/Cys/anti-PTH/BSA/PTH | | 0.615 | |
| Biosensor numbers | $R^2$ | $y$ | Linear ranges (fg/mL) |
| *Reproducibility of the biosensor* | | | |
| 1 | 0.9955 | $16.174x+11.685$ | 10–60 |
| 2 | 0.9929 | $12.155x+0.7913$ | 10–60 |
| 3 | 0.9914 | $12.526x-1.5133$ | 10–60 |
| 4 | 0.9958 | $19.126x+3.6967$ | 10–60 |
| 5 | 0.9870 | $13.852x+4.892$ | 10–60 |
| 6 | 0.9991 | $18.51x+0.685$ | 10–60 |
| 7 | 0.9994 | $30.353x+56.129$ | 10–60 |
| 8 | 0.998 | $32.8x-2.424$ | 10–60 |
| 9 | 0.998 | $30.47x + 21{,}16$ | 10–60 |
| 10 | 0.992 | $28.34x-1{,}524$ | 10–60 |
| **PTH (fg/mL)** | | | |
| Added | Found by the biosensor | Recovery(%)[a] | Relative difference (%) |
| *PTH detection in artificial serum samples* | | | |
| 20 | 21.05 | 105.25 | 5.25 |
| 40 | 41.9 | 104.75 | 4.75 |
| PTH levels (pg/mL) | Found by the biosensor | Found by the reference method | Relative difference (%) |
| *Real sample analysis*[b] | | | |
| Serum | 41.4 | 44.07 | 6.05 |

[a] The recoveries (%) were calculated by the expression (PTH found by the biosensor (fg/mL)/PTH added (fg/mL)) × 100.
[b] The PTH concentrations found by the biosensors were average of three measurements.

and causal circuit. According to this calculation, a value named "goodness of fit" was obtained. Besides, a plot of the relative errors ($\Delta Z/Z$) for the real and imaginary parts of the experimental data was also drawn. In the present anti-PTH biosensor, all steps including preparation of the biosensor and measurement of Kramers–Kronig transforms were performed. The plots of Kramers–Kronig transforms are given in Fig. 5. The goodness of fit values of different biosensor surfaces are also given in Table 1.

For the present impedance based biosensor, obtaining linear, stable, and causal circuit of impedance has a key role in impedance measurements. It was shown that the experimental data agreed with the data obtained by the transform by the help of the Kramers–Kronig transforms performed on the electrochemical impedance spectra related to different biosensor surfaces. Moreover it can be concluded that the impedance spectra obtained were linear, stable, and those of the causal circuit assuming that the biosensor system was not influenced by unknown variables.

A novel impedance technique called single frequency impedance was also applied to the biosensor for the first time in order to characterize the binding of PTH to anti-PTH which was immobilized onto cysteine modified gold electrode surface. Single frequency impedance measures the impedance at a fixed frequency versus time. Consequently it should be possible to control the experiment with repeat time and total time. For this purpose the potentiostat was set up at a fixed frequency, such as 100 Hz. The impedance was measured at this fixed frequency as a function of time and phase angle for 60 min. Fig. 6 shows the single frequency measurement results.

As can be seen from Fig. 6, the single frequency impedance measurements presented notable information about the binding of PTH to anti-PTH. In Fig. 6, the blue curve (upper) shows the change in the impedance as a function of time while the red curve shows the change in the phase angle as a function time. Significant changes in the charge transfer resistance ($\Delta R_{ct}=1106\ \Omega$ in 1 h) and phase angle ($\Delta_{\text{phase angle}}=2.36^{\circ}$ in 1 h) were due to interaction between PTH and anti-PTH. In this experiment, the most important parameter was to pay more attention to prevent environmental interference effects such as a possible electromagnetic wave, an inductive effect from surrounding area, or magnetic stirring of reaction cell that should cause an unstable electrode surface. Eventually, from the results it should be concluded that single frequency impedance can be used for biosensor evaluation,

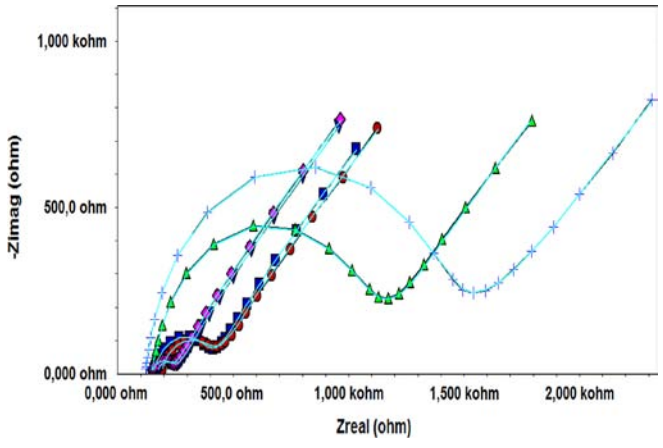


**Fig. 5.** The plots of Kramers–Kronig transforms performed on different layers of the present biosensor. [The turquoise blue lines show Kramers–Kronig transforms performed and fitted on the experimental data and the straight lines show experimental results; -●-●-: bare gold electrode, -▼-▼-: Au/Cys, -◆-◆-:Au/Cys/EDC–NHS, -■-■-:Au/Cys/EDC–NHS/anti-PTH, -▲-▲-: Au/Cys/EDC–NHS/anti-PTH/BSA, -+-+-: Au/Cys/EDC–NHS/anti-PTH/BSA/PTH.] (For interpretation of the references to color in this figure legend, the reader is referred to the web version of this article.)

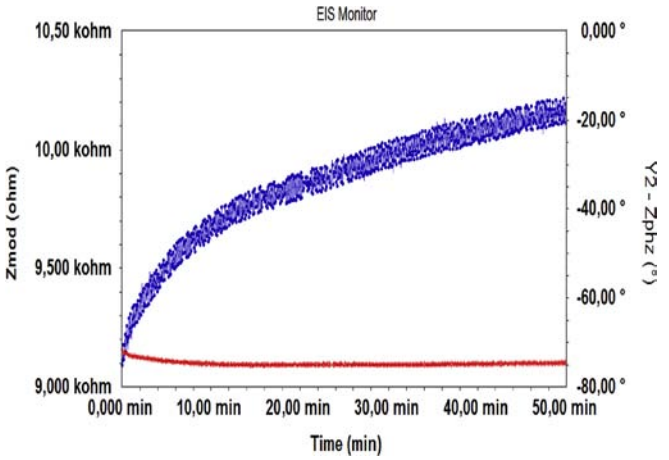


**Fig. 6.** Single frequency impedance measurement. (For interpretation of the references to color in this figure legend, the reader is referred to the web version of this article.)

process monitoring, or to evaluate slow time-dependent changes in a biosensor surface.

The selectivity of the biosensor was investigated by detecting 10 fg/mL of PTH in the presence of several possible coexisting interferences such as aspartic acid, glutamic acid, glycine, cysteine, serum albumine, vascular endothelial growth factor, retinol binding protein, and human epidermal growth factor receptor 3. The impedance ratio was calculated by measuring the impedance of the biosensor in the solution containing 10 fg/mL of PTH and 10 fg/mL of all interfering substances ($I1$) and comparing it with the impedance of biosensor in the solution containing only 10 fg/mL of PTH ($I2$). The degree of interference from the substances can be judged from the values of current ratio. The impedance ratio ($I1/I2$) was calculated as 0.96. From these results, we concluded that the developed biosensor exhibits excellent selectivity towards the determination of PTH, since there was no significant change in the impedance ratio with the interferences.

The biosensor was applied to the artificial serum samples spiked with PTH. Results from 2 different measurements which were averaged can also be seen in Table 1. The results presented here showed that PTH levels of the artificial serum samples analyzed by the present biosensor agreed with that of the artificial serum samples with spiked amount.

Finally, to validate the proposed biosensor, a real human serum sample was tested with a chemiluminescence based analyzer used routinely in the biochemistry laboratories in hospitals (Table 1). Comparison between the two analysis' techniques was made carefully. The results indicated that there were no meaningful differences between the results obtained from the presented biosensor system and the routine method; that is, the concentrations determined by the biosensor and routinely used methods are in good agreement.

## 4. Conclusion

In conclusion, we reported a simple electrochemical biosensor for detection of PTH with ultrahigh sensitivity single frequency measurement which could be an effective method was used for characterization of the interaction between PTH and anti-PTH. Anti-PTH antibody was utilized for the first time in this study for fabrication of an electrochemical biosensor. The immobilization of anti-PTH on Cys modified gold electrodes was significantly simple and ascertained to be effective. The biosensor was fully characterized by CV and EIS in depth. The proposed biosensor is highly reproducible and is able to detect PTH in a linear range of

10–60 fg/mL. The Kramers–Kronig transform was successfully performed on the new biosensor system.

## Acknowledgment

We are thankful for financial support from the Scientific and Technological Research Council of Turkey (TÜBİTAK, Project number: 109 T 172).

## Appendix A. Supplementary material

Supplementary data associated with this article can be found in the online version at http://dx.doi.org/10.1016/j.talanta.2014.02.067.

## References

[1] T.B. Drüeke, Z.A. Massy, Blood Purif. 20 (5) (2003) 494–497.
[2] A.M. Parfitt, J. Bone Miner. Res. 17 (10) (2003) 1741–1743.
[3] T.J. Martin, Trends Endocrinol. Metab. 15 (2) (2004) 49–50.
[4] C. Bieglmayer, G. Prager, B. Niederle, Clin. Chem. 48 (10) (2002) 1731–1738.
[5] A.K. Prahalad, R.J. Hickey, J. Huang, et al., Proteomics 6 (12) (2006) 3482–3493.
[6] L. Jin, S.L. Briggs, S. Chandrasekhar, N.Y. Chirgadze, D.K. Clawson, R. W. Schevitz, D.L. Smiley, A.H. Tashjian, F. Zhang, J. Biol. Chem. 275 (35) (2000) 27238–27244.
[7] S.N. Savvides, T. Boone, P.A. Karplus, Nat. Struct. Biol. 7 (6) (2000) 486–491.
[8] M. Coetzee, M.C. Kruger, South. Med. J. 97 (5) (2004) 506–511.
[9] K. Poole, J. Reeve, Curr. Opin. Pharmacol. 5 (6) (2005) 612–617.
[10] T.M. Murray, L.G. Rao, P. Divieti, F.R. Bringhurst, Endocr. Rev. 26 (1) (2005) 78–113.
[11] P. D'Amour, A. Räkel, J.H. Brossard, et al., J. Clin. Endocrinol. Metab. 91 (1) (2006) 283.
[12] S. Yano, T. Sugimoto, T. Tsukamoto, et al., Kidney Int. 58 (2000) 1980.
[13] S. Cañadillas, A. Canalejo, R. Santamaría, et al., J. Am. Soc. Nephrol. 16 (2005) 2190.
[14] J.P. Bilezikian, A. Khan, J.T. Potts, et al., J. Bone Miner. Res. 26 (10) (2011) 2317–2337.
[15] D. Shoback, N. Engl. J. Med. 359 (4) (2008) 391–403.
[16] J.T. Potts Jr, in: D.L. Kasper, E. Braunwald, A.S. Fauci, et al., (Eds.), Harrison's Principles of Internal Medicine, 16th ed.,McGraw-Hill., New York, NY, 2005, pp. 2249–2268.
[17] A.W. Bott, Curr. Separat. 19 (2001) 71–75.
[18] E. Katz, I. Willner, Electroanalysis 15 (2003) 913–947.
[19] J.G. Guan, Y.Q. Miao, Q.J. Zhang, J. Biosci. Bioeng. 97 (2004) 219–226.
[20] C. Berggren, G. Johansson, Anal. Chem. 69 (1997) 3651–3657.
[21] C. Berggren, B. Bjarnason, G. Johansson, Biosens. Bioelectron. 13 (1998) 1061–1068.
[22] C.A. Malamou, M.I. Prodromidis, Microchim. Acta 163 (2008) 251–256.
[23] C.W.H. Hays, P.A. Millner, M.I. Prodromidis, Sens. Actuators B 114 (2006) 1064–1070.
[24] R. Maalouf, C. Fournier-Wirth, J. Coste, H. Chebib, Y. Saïkali, O. Vittori, A. Errachid, J.-P. Cloarec, C. Martelet, N. Jaffrezic-Renault, Anal. Chem. 79 (2007) 4879–4886.
[25] R. John, M. Spencer, G.G. Wallace, M.R. Smyth, Anal. Chim. Acta 249 (1991) 381–385.
[26] O.A. Sadik, G.G. Wallace, Electroanalysis 5 (1993) 555–563.
[27] O.A. Sadik, M. John, G.G. Wallace, Analyst 119 (1994) 1997–2000.
[28] S. Cosnier, Electroanalysis 17 (2005) 1701–1715.
[29] L. Yang, W. Wei, X. Gao, J. Xia, H. Tao, Talanta 68 (2005) 40–46.
[30] C. Fernandez-Sanchez, C.J. McNeil, K. Rawson, Trends Anal. Chem. 24 (2005) 37–48.
[31] T. Panasyuk-Delaney, V.M. Mirsky, M. Ulbricht, O.S. Wolfbeis, Anal. Chim. Acta 435 (2001) 157–162.
[32] H.B. Fredj, S. Helali, C. Esseghaier, L. Vonna, L. Vidal, A. Abdelghani, Talanta 75 (2008) 740–747.
[33] H.A. Kramers, Phys. Zeits. 30 (1929) 522–523.
[34] R.L. Kronig, J. Opt. Soc. Am. Rev. Sci. Instrum. 12 (1926) 547–557.
[35] M.E. Orazem, B. Tribollet, Electrochemical Impedance SpectroscopyJohn Wiley & Sons, New Jersey, 2008.
[36] W. Ehm, H. Gohr, R. Kaus, B. Roseler, C.A. Schiller, ACH Mod. Chem. 137 (2000) 145–157.
[37] Q.A. Huang, R. Hui, B. Wang, J. Zhang, J. Electrochim. Acta. 52 (2007) 8144–8164.
[38] I. Markovich, D. Mandler, J. Electroanal. Chem. 484 (2000) 194–202.
[39] I. Park, N. Kim, Biosens. Bioelectron. 13 (1998) 1091–1097.
[40] R.K. Mendes, R.S. Freire, C.P. Fonseca, S. Neves, L.T. Kubota, J. Braz. Chem. Soc. 15 (2004) 849–855.
[41] W.U. Dittmer, P. de Kievit, M.W.J. Prins, J.L.M. Vissers, M.E.C. Mersch, M.F.W. C. Martens, J. Immunol. Methods 338 (2008) 40–46.